DRY GAS INJECTION IN FRACTURED CHALK RESERVOIRS - AN EXPERIMENTAL APPROACH

Lars Øyno, Reservoir Laboratories, Norway.
Knut Uleberg, University of Trondheim, NTH.
Curtis H. Whitson, University of Trondheim, NTH.

ABSTRACT

Gas injection in fractured chalk reservoirs has sometimes been regarded as inefficient due to early breakthrough of injection gas. However, if the pressure in the reservoir is increased, and a non-equilibrium dry gas is injected into the fracture system, compositional effects will be active between the gas in the fractures and oil in the matrix. The method is potentially well suited to fractured chalk reservoirs in the Ekofisk Area in the North Sea due to relatively small block sizes (10-100 cm). Furthermore, some of the chalk reservoirs have been waterflooded, and some are still in the primary depletion phase.

Laboratory experiments have been conducted on composite cores at reservoir conditions using recombined reservoir fluids to investigate the potential of secondary and tertiary recovery using gas injection. Gas was injected into a fracture/chalk system at different initial water saturations for pressures above the bubble point of the in-situ oil.

Results from experiments and simulation conducted on composite cores up to 60 cm long indicate that compositional effects contribute to considerable additional oil recovery. Gravity drainage has previously been regarded as an important recovery mechanism in this type of gas injection. Gravity drainage and capillary redistribution due to low IFT controls the final oil saturation in the core during gas injection. The time required to reach capillary/gravity equilibrium depends on oil/gas density difference, gas/oil IFT (absolute value and IFT gradients with depth), and molecular diffusion in both gas and oil phases.

INTRODUCTION

Interest in gas and water injection in the Ekofisk area offshore Norway has resulted in numerous laboratory studies to quantify oil recovery by different EOR process. The laboratory studies have primarily concentrated on water imbibition [1-5] during the 1970s and 1980s and nitrogen injection[6,7] in the 1980s. Most imbibition tests have been conducted at atmospheric pressure, and at temperatures from lower than reservoir temperatures.

Two pilot water injection projects in the Ekofisk Field confirmed the applicability of water injection in the Ekofisk fractured chalk. Large-scale water flooding is now ongoing in the Ekofisk Field [8-10]. Even though the water flooding projects have been successful, considerable oil will be left behind following water flooding. This residual oil after spontaneous and gravity-assisted water imbibition is the target of studies of tertiary gas injection.
Several simulation studies conducted by oil companies in the Ekofisk area have considered "massive" gas injection in the Ekofisk Field and other fields such as Eldfisk. In these studies, substantial quantities of gas are injected to increase the reservoir pressure from current

conditions to higher pressures. The recovery mechanisms of high-pressure gas injection are complicated, and several major uncertainties have been identified in reservoir models trying to simulate the displacement process. For example, at higher reservoir pressures the gas-oil interfacial tension (IFT) is reduced substantially and capillary/gravity drainage can produce significant incremental oil. However, diffusion-controlled vaporization by a lean gas injection increases the IFT again. These two effects thus act against each other.

The aim of the work described in this report is to investigate the effect of increased gas pressure in the fracture network. The experimental work provides data for numerical simulation studies enabling us to understand the recovery mechanisms and predict production with different boundary conditions, block sizes, and more realistic "field" time scales.

EXPERIMENTAL PROCEDURES

Core Samples

Core samples of outcrop Liege chalk were cut 5 cm long and 1.5" in diameter. The chalk is very homogenous and has a gas permeability between 2.5-3 mD. The porosity is between 42-44%, close to values for Maastrichtian chalk in the Ekofisk fields. The core plugs were cleaned by flooding methanol and toluene at 70°C. Solvents were removed by evaporation in an oven, and porosity was measured on the single plugs. The cores were then saturated with synthetic Ekofisk brine and S_{wi} was established in each plug using a centrifuge with air as the displacing fluid. Pore size distribution of the outcrop chalk is shown in Fig. 1. In one experiment, Maastrichtian chalk from the Ekofisk Field was used. Details concerning cores and initial conditions are found in Table 1. The cores were mounted on top of each other to provide one single composite core. Capillary continuity between the cores was improved using kaolinite powder between the core plugs.

Experiments

The core holder's inside diameter is 40 mm, and the core diameter is 37 mm, rendering an annulus of 1.5 mm around the core, simulating a "fracture". The core is exposed to gas from all sides, and the relatively large width of the fracture ensures a negligible pressure gradient along the core when circulating fluids through the core holder. The produced fluids are collected and measured at reservoir conditions in a high pressure separator.

Recombination of oil and gas was carried out by injecting Ekofisk separator gas into the core holder and separator system (see Fig. 2). A predetermined amount of Ekofisk separator oil was then injected into the system. Pressure was monitored, and the oil/gas mixture was circulated in the system to speed up equilibrium. Once pressure had stabilized, a bubblepoint was measured on the oil inside the core holder and pore system. Bubblepoint values close to current Ekofisk pressures (3700-4200 psi) were obtained.

After the bubble point measurement, separator gas was injected into the fracture, and the system pressure was increased to 6000 psia. This simulated a gas pressure build-up in the fracture network. The oil and water production was measured while circulating the gas in the system.

For tertiary recovery experiments, spontaneous imbibition was carried out in the core holder prior to gas injection. Water was circulated around the core until all movable oil was produced.

An extensive study of PVT characteristics and EOS calculations have been carried out on the recombined Ekofisk fluids. The swelling and vaporization potential of the fluids was particularly important to determine, and some of the results from this work can be found in Fig. 3. Table 2 shows the composition of the separator oil and gas, and the final recombined oil.

EXPERIMENTAL RESULTS

Experiments have been performed at several initial conditions of water saturation in the cores. Fig. 4 shows spontaneous imbibition results in two of the tests. These results show normal imbibition behavior for chalks, and similar imbibition to what is observed in more water wet regions of the North Sea chalk fields.

Fig. 5 shows free oil and water observed in the separator in three of the gas injection tests. Notice that very little oil is observed. Note also that some water is produced in the experiments with high water saturations. This water amount corresponds closely to the volume increase of oil calculated by swelling, and indicates that the trapped oil swells, but free water produces from the matrix. Fig. 6 shows the capillary pressure curve for the outcrop cores used in the experiments.

Fig. 7 shows results from a gas injection experiment with S_{wi} in the cores (Experiment 4), where small gas samples were taken during the equilibration period. The results show that only a few days are required for the gas to be significantly enriched. The system in this experiment has a $V_{gi}/V_{oi}=1.9$ (see Fig. 3). Production of this gas will thus result in an oil recovery of 30% of OOIP. Compositions of the gas samples are shown in Table 1.

SIMULATION RESULTS AND DISCUSSION

One of the secondary gas injection experiments was simulated using a fully implicit compositional simulator (SSI's COMP4) that accounts for molecular diffusion and dynamic IFT-scaled capillary pressure. The actual laboratory model was simulated (to the extent possible), so quantitative results could be compared with experimental data.

Furthermore, a mechanistic study of the recovery process was made. Some of the results from this study are also presented here to understand discrepancies in calculated and measured results, and to help justify some of our recommendations for future work.

Model Specifications

A two-dimensional radial grid was used. Two model regions were defined: (1) the stack of cores and (2) the surrounding "fracture" volume (including the separator volume). Radial grids in the core region were chosen so that each grid had equal area in the horizontal plane. The final runs were made using nine radial grids in the core region. Four equal-size vertical grids were used for each of the 13 core plugs, resulting in a total grid dimension for the core region of 9x52.

The fracture region was modeled with one outer radial grid, one layer above the core region, and three layers below the core region: (i) a thin layer representing the fracture (similar to the upper fracture layer), (ii) a layer with dead volume in the innermost 9 radial grid and "open" in the outer radial grid, and (iii) a lower layer that represented the separator volume. All fracture-region layers had ten radial grid, nine of which were the same dimension as the core-region radial grids.

The fracture cells used zero capillary pressure and straight-line relative permeabilities with zero endpoint saturations. Core-region capillary pressure was taken from air-water centrifuge experiments, fit to a Corey-type equation,

$$P_c = P_{ce} S_{Le}^{-1/\lambda} + (P_{ca} - P_{ce}) \bullet 10^{\beta(S_{Le}-1)} \quad (1)$$

where $S_{Le}=(S_o-S_{org})/(1-S_{wi}-S_{org})$, and $S_{wi}=S_{org}=0.1$. The original Corey parameters in Eq. 1 are $\lambda=2.42$ and $P_{ce}=1.413$ bar (for a reference air-water IFT $\sigma=50$ mN/m). Parameters in the extension of the Corey equation (second term of Eq. 1) are $P_{ca}=0$ and $\beta=25$; simulations presented in this paper use $P_{ca}=P_{ce}$. Fig. 6 shows the Corey curves and measured capillary pressure data from one of the core samples.

Relative permeability curves were generated from Corey-type equations based on model parameters determined from the capillary pressure data,

$$k_{ro} = S_{Le}^{(2+3\lambda)/\lambda} \quad (2)$$

$$k_{rg} = (1 - S_{Le})^2 \, (1 - S_{Le}^{(2+\lambda)/\lambda}) \quad (3)$$

Gas-oil capillary pressures in the model were scaled linearly with gas-oil IFT,

$$P_c = P_{c(reference)} \frac{\sigma_{go}}{\sigma_{reference}} \quad (4)$$

where σ_{go} is calculated at each grid cell in the model using the parachor method,

$$\sigma_{go}^{1/4} = \sum_{i=1}^{N} P_i \left(\frac{\rho_o}{M_o} x_i - \frac{\rho_g}{M_g} y_i \right) \quad (5)$$

The simulator also computes IFT for single-phase oil cells using compositions from the oil's bubblepoint calculation; densities are calculated at the cell pressure ($p>p_b$). Though non-physical, this single-phase IFT is required to ensure that gas has the possibility to enter from a gas-filled fracture to an oil-filled core cell (when gravity is sufficient to overcome the IFT-corrected capillary pressure).

Physically, the mechanism for gas entering from a fracture to an undersaturated oil would require an ultra-thin contact volume (grid cell) at the fracture/matrix interface. In this volume, oil would immediately become saturated with fracture gas. (Oil volume expansion due to

swelling would cause a small amount of free oil to enter the fracture, either being dissolved completely into the fracture gas, or moving as a free phase in the fracture together with the fracture gas). The swollen oil in the contact volume would be saturated at reservoir pressure, and this saturated system's IFT would be the most correct value to use for modelling. The approximate single-phase IFT used in the simulator will usually overestimate the true saturated IFT, but the calculation is much faster than would be required for a more rigorous estimate.

PVT calculations were made using a seven-component pseudoized EOS characterization (Table 3), including three C_{7+} fractions.

Model Results and Interpretation

Two simulations of Experiment No. 4 are presented below, together with an interpretation of the recovery mechanisms associated with this one experiment, and some implications for the general behavior of high-pressure gas injection in fractured chalk. The two simulations are referred to as Diffusion Case and No-Diffusion Case.

Physically, molecular diffusion will always exist when gas is injected in a fractured reservoir, and we expected our experiments to be influenced strongly by diffusion in the gas phase and the oil phase. The Diffusion Case used the simulator's default diffusion formulation based on the modified Sigmund[11] correlation presented by da Silva and Belery.[12] These correlations have been verified for Ekofisk oil/gas systems using a specially-designed diffusion experiment and numerical simulator.[13]

The Diffusion Case is our best interpretation of the actual experiment, and though the measured data are very limited, we feel that the simulated results give an accurate description of the true physical process of recovery for this particular experiment. We also feel that the recovery mechanisms observed in this experiment are representative of localized matrix/fracture processes that should occur with field-scale gas injection in fractured chalk.

The No-Diffusion Case was run to help understand the role of molecular diffusion in the recovery process. Furthermore, the recovery mechanisms observed in the absence of molecular diffusion probably give a reasonable description of what actually occurs in the part of a reservoir where the first fracture gas to enter is already saturated from previous matrix/fracture interactions (gas diffusion becomes small, and oil diffusion is only important if effective block heights are small and gravity drainage is negligible).

Fig. 7 shows the average composition of gas in the fracture system (annulus/separator volume) as a function of time for the Diffusion Case. Measured gas compositions from two samples that were collected at 4 and 8 days are also shown. The simulated results are consistent with measured data (particularly for C_{7+}).

Fig. 8 shows simulated oil recovery versus time resulting solely from the enrichment of fracture gas (free oil in the fracture/separator volume was not seen experimentally or in the simulated Diffusion Case). Recovery is expressed as cumulative STO "vaporized," calculated by passing the fracture gas composition through a single stage flash (recall that the laboratory system is

actually closed throughout the experiment). The approach to 30% recovery of OOIP is consistent with equilibrium PVT calculations made prior to the experiment (see Fig. 3); the initial gas-to-oil volume ratio was $V_{gi}/V_{oi}=1.9$.

Fig. 9 shows simulated average oil saturation in the core stack as a function of time. For the Diffusion Case, desaturation occurs rapidly, whereas oil desaturation for the No-Diffusion Case starts much slower.
Also shown on Fig. 9 is the theoretical desaturation value that would be expected by a pure diffusion/vaporization process (in the absence of gravity drainage and with no free oil production to the fracture/separator volume). The average saturation of 69% was calculated for a closed system where the initial contents of matrix and fracture were flashed at the system pressure (6000 psia and 270°F). Because a small amount of makeup gas had to be injected to maintain system pressure during the simulations, the overall system composition became somewhat leaner and the final equilibrium condition at 150 days gave a theoretical average oil saturation of 62%.
Fig. 9 shows the theoretical desaturation limits for capillary/gravity equilibrium using (1) a final system equilibrium IFT of 0.2 mN/m (and corresponding densities), and (2) the minimum IFT of 0.025 mN/m (and corresponding densities) observed late in the No-Diffusion simulation.

Fig. 10 and 11 show the desaturation profile along the core stack for the Diffusion Case, together with the profiles of gas-oil IFT. These figures show a complicated recovery process where a gas front develops, moves downward rapidly, and slows to a stop as the front reaches the capillary height.

The frontal IFT is initially quite low. However, a strong gradient in gas composition develops behind the gas front by diffusion in the gas phase. This compositional gradient causes a severe IFT gradient that imbibes oil upwards. Consequently, the net oil desaturation is significantly reduced compared with what would have been achieved in the absence of the IFT gradient.

Fig. 14 shows capillary/gravity equilibrium curves calculated using frontal IFT and density differences for the Diffusion Case. The simulation saturation profile at 150 days is also shown. Once the gas front slows down and stops at the entry height, gravity drainage and diffusion-controlled vaporization continue to desaturate or redistribute saturation in the core. However, this process is too slow to be modeled in this simulation.

Figs. 12-13 show saturation and IFT profiles for the No-Diffusion Case. A gas front also develops in these simulations, but the frontal IFT reaches and maintains a very low value (<0.03 mN/m) after about 10 days. The IFT gradient behind yhe front is not strong enough to avoid a piston-like diplacement of oil.

Recovery Mechanisms

For the experiments we have simulated, the mechanisms of oil production from the core stack to the fracture appear to involve the following processes. We feel that these processes will also exist locally in actual gas injection projects in fractured chalk reservoirs.

1. At early times, gas enters from the fracture to the matrix by gravity overcoming capillary retention. The gas dissolves in the undersaturated oil and swells the oil. Swelling forces oil production from the core.

   For gas to enter an undersaturated oil-filled matrix block by diffusion alone (in the absence of gravity, where entry height is larger than effective block height), it is necessary to initiate the diffusion process in the oil-filled matrix block. Physically, a thin matrix layer can be used around the core, initialized with a two-phase saturated gas/oil mixture. Capillary pressure in the thin layer must be large enough to avoid gas entering by gravity.

2. The matrix oil that has been partially (or completely) saturated with gas has a different composition than the original oil. This compositional difference causes molecular diffusion of all components (primarily methane) in the oil phase. However, this process appears to be unimportant in the short time scale of these experiments.

3. As gas continues entering the oil-filled matrix, a free gas saturation eventually develops. Oil is displaced from the core to the fracture as gas enters by gravity. Gas continues to enter the matrix block until capillary forces balance the gravity forces.

4. For a relatively lean fracture gas, the free equilibrium gas in the matrix is richer in heavier components than the fracture gas. This results in production of heavier components from the matrix to the fracture by diffusion in the gas phase. A strong compositional variation with depth develops in the matrix block as a result of diffusion in the gas phase. This compositional variation causes a strong variation of gas-oil IFT with depth. The IFT gradient may be strong enough for imbibition of oil upwards against gravity, thereby reducing the net oil produced by the incoming gas.

5. For a relatively rich fracture gas, diffusion will play only a small role in the recovery process. Displacement by gravity drainage will occur with very low IFTs at the gas front.

6. Recoveries from diffusion-controlled vaporization by lean gas, in the absence of gravity drainage can potentially result in significant incremental recoveries at sufficiently high pressures. Injection of 1 to 2 pore volumes of lean injection gas can potentially recover 15 to 30% of oil in place.

Our results have the inherent limitation of not having simulated the actual fracture system realistically. Capillary continuity between matrix blocks, fracture/matrix geometries, reimbibition, and several other issues have also been neglected. da Silva and Meyer[14,15] give an excellent treatment of these issues in an earlier simulation study. Yet other issues remain unsolved, including the dynamics of fracture composition as a function of time and space in an actual full-field gas injection project.

CONCLUSIONS

1. Lean gas injection at elevated reservoir pressure offers a significant oil recovery potential in fractured chalk reservoirs. Although water injection will probably continue to be the main secondary recovery process used in chalk reservoirs, gas injection may still be a viable alternative for some reservoirs as a secondary recovery method. It also appears that high-pressure gas injection may be feasible as a tertiary recovery method for waterflooded chalk reservoirs.

2. As a secondary recovery process in fractured chalk reservoirs, lean gas injection at high pressure may result in significant incremental recoveries, depending mostly on effective block height, *developed* gas-oil IFTs and IFT gradients in the matrix blocks, and *developed* fracture gas composition. The recovery mechanism may be strongly effected by molecular diffusion in the gas phase in the matrix blocks.

3. For injected gas volumes greater than about 0.5 HCPV, significant (>10%) recoveries of remaining oil in place can be produced by pure vaporization. This applies to both secondary and tertiary processes, though the time scale for recovery in tertiary processes is probably slower, and has not yet been quantified.

FURTHER WORK

The presented results represent the first part of a study where secondary and tertiary massive gas injection in fractured chalk reservoirs are examined. Experiments are ongoing where gas samples are taken during tertiary gas injection (after spontaneous imbibition). The results are promising for these results as well.

ACKNOWLEDGMENTS

We would like to thank the participants in the GAS and WAG subprojects in the RUTH Program, the Norwegian Research Council, and the participating oil companies. We thank Phillips Petroleum Company Norway for providing oil samples and core material for this work, and for helpful discussions during this project. Finally, we would like to thank the laboratory staff at ResLab for performing the experiments, as well as J. Kleppe and Ø. Fevang at NTH for helpful comments.

NOMENCLATURE

M_g = Molecular weight of gas
M_o = Molecular weight of oil
N = Stock-tank oil (STO) in place, cm^3
N_p = Produced STO, cm^3
P_c = Capillary pressure, bar
P_{ca} = Actual entry capillary pressure, bar
P_{ce} = Corey entry capillary pressure, bar
P_i = Parachor for component i
S_{wi} = (Initial) Irreducible water saturation
S_o = Oil saturation
S_{org} = Residual oil saturation to gas
S_{orw} = Residual oil saturation to water
V_{gi} = Volume of gas in fracture system, cm^3
V_{oi} = Initial volume of oil in matrix (reservoir conditions), cm^3
x_i = Oil molar composition
y_i = Gas molar composition
β = Extended Corey capillary pressure parameter
λ = Corey pore size distribution parameter
σ = Interfacial tension (IFT), mN/m
ρ_o = Oil density, kg/m^3
ρ_g = Gas density, kg/m^3

REFERENCES

1. Gunlikson, R.D. and Wier,D.R.(1985): "Laboratory Studies on Water Imbibition in "Ekofisk". Chalk Research Program Symposium, Stavanger.
2. Johansen,M. and Hjelmeland,O.(1990): "A Study of Eldfisk Chalk Imbibition Characteristics". Presented at 3rd North Sea Chalk Symposium, June 11 - 12, Copenhagen, Denmark.
3. Torsæter, O. (1984): "An Experimental Study of water Imbibition in Chalk from the Ekofisk Field", paper 12688 presented at the SPE/DOE Symposium on Enhanced Oil Recovery, Tulsa, OK.
4. Øyno,L. and Hjelmeland, O.: "Relative Permeability as a Function of Reservoir Depletion/Well Drawdown. ". Report issued under the Joint Chalk Research Program, phase III, project 3 (Jul. 1992).
5. Vidal,J. (1990): "Determination of Characteristics of Ekofisk Formations by forced and spontaneous Experimental Waterflooding". Presented at 3rd North Sea Chalk Symposium, June 11 - 12, Copenhagen, Denmark.
6. Thomas, L.K. et al.: "Ekofisk Nitrogen Injection", paper SPE presented at the 1989 SPE Annual Technical Conference and Exhibition, San Antonio, Oct. 8 - 11.
7. da Silva, F.V.: "Primary and Enhanced Recovery of Ekofisk Field - A Single - and Double - Porosity Numerical Simulation Study", paper SPE 19840 presented at the 19891 SPE Annual Technical Conference and Exhibition, San Antonio, Oct. 8 - 11.

8. Dangerfield, J.A. and Brown, D.A. (1985): "The Ekofisk Field". Presented at North Sea Oil and Gas Reservoirs. The Norwegian Institute of Technology (Graham & Trotman, 1987),pp. 3 - 22.
9. Sulak, R.M., Nossa, G.R. and Thompson, D.A.: "Ekofisk Field Enhanced Recovery", North Sea Oil and Gas Reservoirs - II, Norwegian Inst. of Technology, Graham and Trotman, London (1990) 281 - 95.
10. Sulak, R.M.: "Ekofisk Field: The first 20 Years", JPT (Oct. 1990) 1265 - 71.
11. Sigmund, P.M.: "Prediction of Molecular Diffusion At Reservoir Conditions. Part I - Measurement and prediction of Binary Dense Gas Diffusion Coefficients," J. Can. Pet. Tech. (April-June 1976) 48-57.
12. da Silva, F.V. and Belery, P.: "Molecular Diffusion in Naturally Fractured Reservoirs - A Decisive Recovery Mechanism," paper SPE 19672 presented at the 1987 SPE Annual Technical Conference and Exhibition, San Antonio, Oct. 8-11.
13. Christoffersen, K.: "High-Pressure Experiments with Application to Naturally Fractured Chalk Reservoirs. 1. Constant Volume Diffusion. 2. Gas-Oil Capillary Pressure," dr.ing. thesis, U. Trondheim, NTH (1992).
14. da Silva, F.V. and Meyer, B.: "Analysis of Gravity-Capillary Equilibrium in Chalk Fractured Reservoirs," Third Chalk Research Symposium, Copenhagen, June (1990).
15. da Silva, F.V. and Meyer, B.: "Improved Formulation for Gravity Segregation in Naturally Fractured Reservoirs," Sixth European Symposium on Improved Oil Recovery, Stavanger, May (1991).

TABLE 1. Experimental summary and core properties.

Experiment No.	Water Saturation Before Gas Inj.	Cores	Porosity (%)	S_{wi} (%)	S_{orw} (%)	Length (cm)	Diameter (cm)
1	$1-S_{orw}$	Ekofisk	31.6	18.9	28.0	36.5	3.77
2	S_{wi}	Outcrop	43.6	23.3	-	38.2	3.77
3	$S_{wi} < S_w < 1-S_{orw}$	Outcrop	42.6	20.2	38.8	51.6	3.77
4	S_{wi}	Outcrop	42.4	18.7	-	51.7	3.77

TABLE 2. Molar compositions of fluids used in and sampled during the experiments.

	All Experiments			Experiment 4		
Component	Separator Gas	Separator Oil	Recombined Oil	Gas Sample 1	Gas Sample 2	Gas Sample 3
N_2	0.36	0.00	0.19	0.25	0.09	0.30
CO_2	2.01	0.47	1.28	1.87	1.74	1.79
C_1	82.50	11.29	49.51	83.76	83.01	79.26
C_2	8.73	4.02	6.51	8.68	8.04	8.41
C_3	3.57	3.97	3.64	3.37	2.90	3.61
iC_4	0.50	1.09	0.76	0.45	0.41	0.53
nC_4	1.17	3.48	2.20	0.97	0.94	0.96
iC_5	0.31	1.90	1.03	0.22	0.23	0.48
nC_5	0.39	2.85	1.50	0.23	0.27	0.66
C_6	0.29	4.79	2.34	0.14	0.28	0.89
C_{7+}	0.78	66.14	31.04	0.06	2.09	3.11
	100.00	100.00	100.00	100.00	100.00	100.00
Bubblepoint (bara)			295			
GOR (Sm^3/Sm^3)		25.5	141			
Time (days)				0.02	4	7.8

TABLE 3. SRK EOS properties and compositions.

Comp.	Mol Weight	Critical Temp. (R)	Critical Pressure (psia)	Acentric Factor	Specific Gravity	EOS Constant Multipliers Omega A	Omega B	Volume Shift s=c/b	Critical Volume (ft3/mol)	Parachor
C1N2	16.09	342.3	666.6	0.0117	0.3307	1.0019	1.0001	0.02289	1.5889	76.9
C2CO2	32.36	549.3	788.9	0.1221	0.4616	1.0183	1.0529	0.06264	2.1763	101.8
C3C4	50.39	713.2	579.5	0.1676	0.5421	0.9785	0.9904	0.08783	3.6965	167.1
C5C6	78.89	877.9	461.8	0.2699	0.6466	0.9921	0.9968	0.13120	5.4315	249.1
C7P1	134.43	1082.5	359.7	0.5948	0.7967	0.9659	0.9916	0.14138	10.7281	404.0
C7P2	271.84	1333.2	230.6	0.9386	0.8683	0.9693	0.9870	0.11686	18.0178	721.8
C7P3	517.81	1672.2	198.0	1.2676	0.9376	0.9490	0.9800	-0.11543	22.9861	1065.4

	Binary Interaction Parameters C1N2	C2CO2	Molar Compositions Original Oil z	Inj. Gas y
C1N2			0.4970000	0.8346
C2CO2	0.336E-01		0.0779000	0.1069
C3C4	0.533E-03	0.335E-01	0.0660000	0.0490
C5C6	0.533E-03	0.335E-01	0.0487000	0.0079
C7P1	0.107E-02	0.335E-01	0.1706488	0.0016
C7P2	0.107E-02	0.335E-01	0.1016343	0.0000
C7P3	0.107E-02	0.335E-01	0.0381168	0.0000

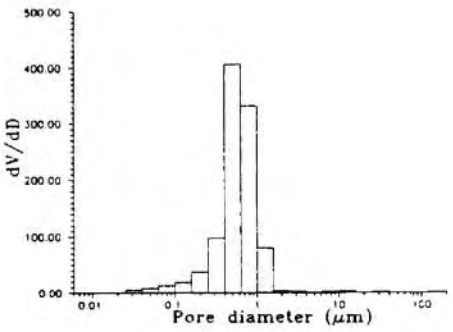

Fig. 1 Typical pore size distribution for Ekofisk chalk.

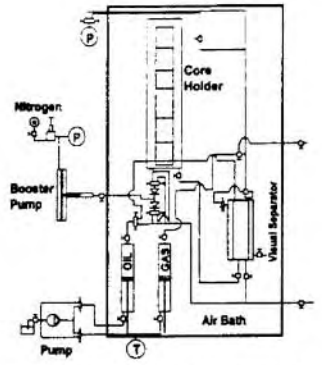

Fig. 2 Schematic of high-pressure experimental equipment.

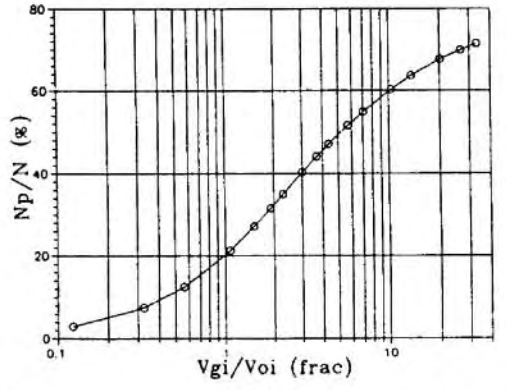

Fig. 3 STO recovery of OOIP at start of gas injection for pure vaporization process (no gravity drainage).

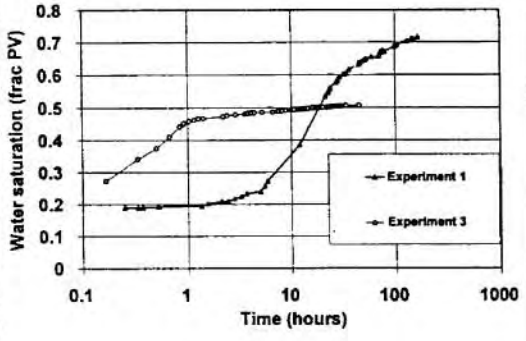

Fig. 4 Spontaneous imbibition test at reservoir conditions.

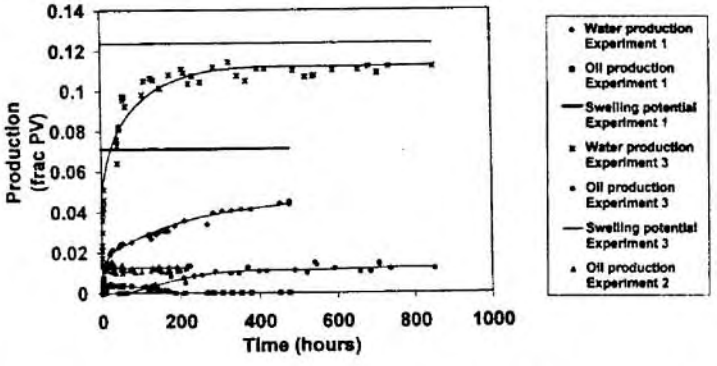

Fig. 5 Free oil and water production at reservoir conditions from increase in pressure during gas injection.

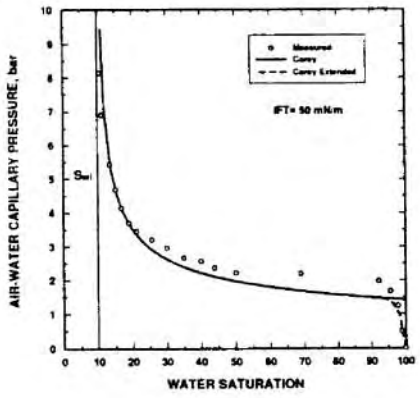

Fig. 6 Capillary pressure curves for chalk samples in Experiment 4.

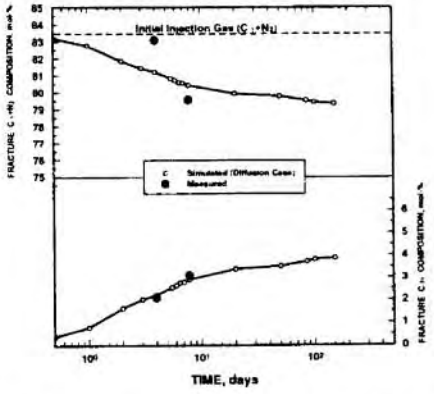

Fig. 7 Fracture gas composition as function of time. Measured and Diffusion Case simulation results.

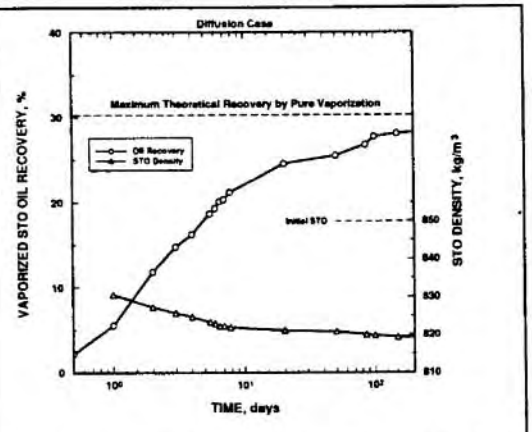

Fig. 8 Vaporized STO recovery and density versus time from flash of fracture gas. Diffusion Case simulation results.

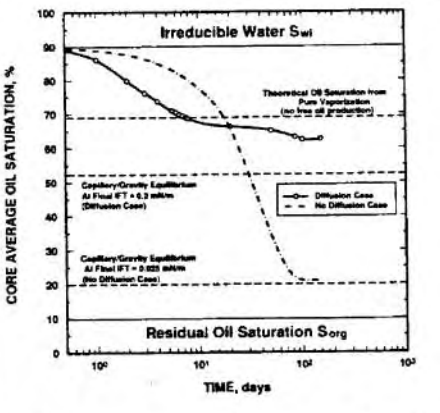

Fig. 9 Average oil saturation in core stack as function of time. Diffusion and No-Diffusion Cases. Limiting saturations for pure vaporization, and capillary/gravity equilibrium.

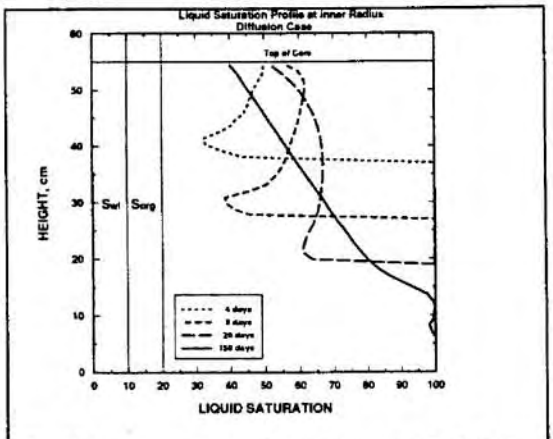

Fig. 10 Liquid saturation profile at various times for Diffusion Case simulation. Saturations at innermost radial grid.

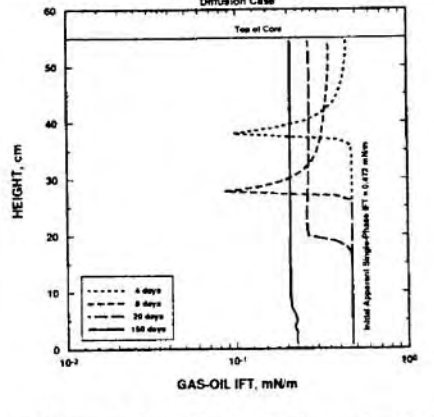

Fig. 11 Gas-oil IFT profiles as function of time for Diffusion Case simulation. IFT values at innermost radial grid.

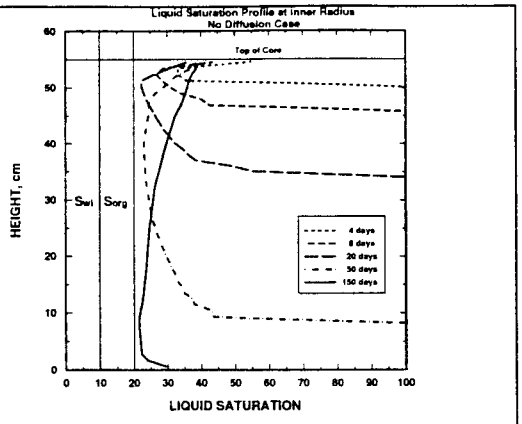

Fig. 12 Liquid saturation profiles at various times for No-Diffusion Case simulations. Saturations at innermost radial grid.

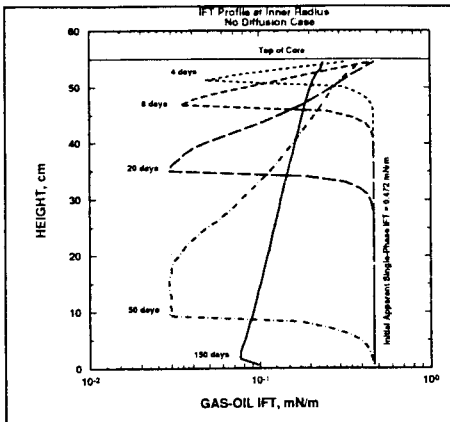

Fig. 13 Gas-oil IFT profiles at various times for No-Diffusion Case simulations. IFT values at innermost radial grid.

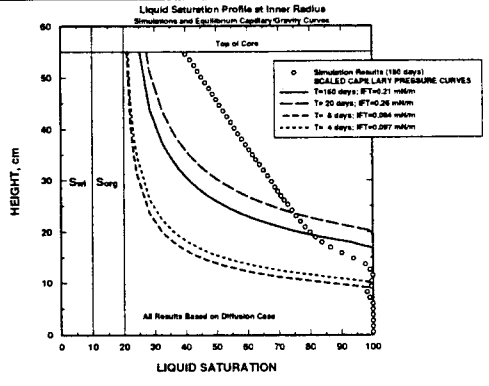

Fig. 14 Liquid saturation profiles for Diffusion Case simulation at 150 days. IFT-scaled capillary/gravity equilibrium profiles based on IFTs and density differences at gas front at various times.

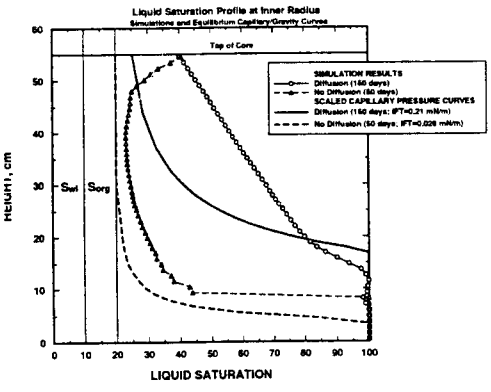

Fig. 15 Liquid saturation profiles for Diffusion and No-Diffusion Cases at late times. IFT-scaled capillary/gravity equilibrium profiles based on IFTs and density differences at gas front from the two Cases.